Comparative Study of a Turbulent Wall-Attaching Offset Jet and a Plane Wall Jet

Soon Hyun Yoon*, Kyung Chun Kim*, Dae Seong Kim* and Myung Kyoon Chung**

(Received September 7, 1992)

The flow field characteristics of a two-dimensional wall-attaching offset jet(WAOJ) are experimentally investigated by comparing with those of a turbulent plane wall jet(PWJ). The mean velocity, the turbulent stresses and triple velocity correlations are measured with a split film probe and an X wire probe. Even with the strong influence of the suction pressure field in the recirculation bubble at the lower corner, it is found that the WAOJ in the wall jet region has a close similarity with the PWJ. Especially, the decay of maximum velocity and the upper jet spread along the maximum velocity line of the WAOJ are virtually the same as those of the PWJ. The mean velocity profile of the WAOJ attains similarity after the jet impingement onto the lower plate. However the profiles of second and third-order moments of fluctuating velocities vary rapidly before the impingement and then relax very slowly to the similarity profiles of the PWJ.

Key Words: Wall-Attaching Offset Jet, Recirculation Bubble, Reattachment Region, Impingement Process, Wall Jet Region

1. Introduction

When a plane turbulent air jet is discharged into quiescent surroundings above a plate offset from and parallel to the axis of the jet discharge, air entrainment through the free boundary below the jet and above the plate reduces the pressure in this region, forcing the jet to deflect towards the wall boundary and eventually attach to the plate wall. After impingement of the jet, the flow redevelops on the plate wall with the downstream distance. The general flow field is schematically depicted in Fig. 1(a). This kind of flow phenomenon has been variously called a reattached wall jet (Rajaratnam and Subramanya, 1968), a reattaching jet (Sawyer, 1963), a wall-attaching jet (Tritton, 1977), or an offset jet (Hoch and Jiji, 1981). In the present study, a more descriptive name "wall-attaching offset jet"(hereinafter refer to as WAOJ) is adopted.

The WAOJ is frequently found in many engineering devices; examples are the cooling of a combustion chamber wall in a gas turbine, the use of an air deflector as a circulation controller, the automobile demister, and an air jet discharge for environment control. Because of its importance, there are a number of experimental and theoretical studies which have been surveyed in detail by Pelfray(1984).

Previous investigations have been concerned mostly with mean flow characteristics. Early works by Bourque and Newman(1960) and Sawyer(1960, 1963) showed that the wall pressure distribution and the reattachment location depend largely on the offset height to the jet width ratio, H/D, for flows with high Reynolds numbers ($Re_D > 2.3 \times 10^3$, based on the jet width), which

* Department of Mechanical Design Engineering, Research Institute of Mechanical Technology, Pusan National University, Pusan, 609-735, Korea
** Department of Mechanical Engineering, Korea Advanced Institute of Science and Technology, Daejon, 305-701, Korea

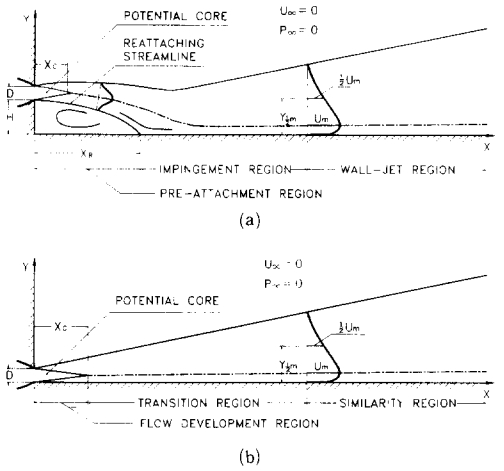

Fig. 1 Definition sketch of (a) the wall-attaching offset jet and (b) the plane wall jet

was later confirmed by Kumada et. al.(1973). In the experiments of Nozaki et. al.(1981), it was found that the reattaching flow field depends further on the initial turbulence intensity and that the dependency diminishes as the turbulence intensity becomes larger. Recently, Pelfray and Liburdy(1986a) provided a detailed experimental description of the mean velocity field in the pre-attachment and impingement regions. And they discussed in depth the effects of curvature strain rate on the jet spread, the maximum velocity decay, and the entrainment. An integral analysis based on an entrainment model was presented by Hoch and Jiji(1981) to predict the jet trajectory, the reattachment length, the wall pressure distribution, and the maximum axial velocity decay. They also compared the predictions with their experimental data with a reasonable success.

The downstream development after the wall attachment has also been studied by several investigators (Parameswaran and Alpey, 1975; Rajaratnam and Subramanya, 1968). They found that the mean flow field in this region is much similar to the classical wall jet with virtually no dependence on the offset ratio.

Turbulence data on the WAOJ are, however, very limited. To the authors' knowledge, the works by Pelfray and Liburdy(1984, 1986b) are the only available experimental studies on the turbulence structure of the WAOJ. They presented representative energy spectra, integral scales and fluctuating velocity components u' and v' along the jet centerline and dividing streamline (Pelfray and Liburdy, 1984), and distributions of u' and v' within the pre-attachment region only (Pelfray and Liburdy, 1986b). Therefore, more turbulence data are needed in wider flow field, including the wall jet region, in order to be used by turbulence modellers to evaluate the performance of various computational models for complex turbulent flow with the high curvature of streamlines in the initial development region.

The present study is aimed at obtaining turbulence data of the WAOJ in the whole region of interest, ranging from the pre-attachment region to the wall jet region far downstream. The observed characteristics of the mean velocity field are compared with those of other WAOJs. In addition, the mean velocity field and the turbulence data in the WAOJ are discussed in comparison with the data of the plane wall jet (hereinafter refer to as PWJ) in order to find any influence of the high curvature of the streamlines in the pre-attachment region on the downstream development of the turbulence structure. Here, the flow configuration of the PWJ was obtained by raising the lower plate up to the lower edge of the nozzle (Fig. 1(b)).

2. Experimental Set-Up

The experiment was conducted in a low speed open-return wind tunnel. Compressed air was supplied by a 5 HP centrifugal fan. The wind tunnel consists of a diffuser, plenum chamber and a contraction nozzle. The shape of the contracting wall was designed by smoothly combining two cubic curves as recommended by Morel(1977). The contraction ratio is 25 : 1 and the exit nozzle has dimensions of 800 mm $\times$ 20 mm.

Variation of the exit velocity in the lateral direction was within 2.3%, and that in the crosswise direction was within 1.5%. All of the experiments were performed with the exit velocity of 30 m/s (Re_D=39000) and the initial turbulent intensities at the exit were u'/U_J=0.001, v'/U_J=0.002

and $w'/U_J=0.0015$, where u', v' and w' are rms velocity components in streamwise, crosswise and lateral directions, respectively, and U_J is the mean velocity at the nozzle exit. The boudary layer at the jet exit was laminar with the momentum thickness Reynolds number $Re_\theta \simeq 270$, which implies that the exit boundary layer is fully developed (Cebeci and Bradshaw, 1977).

The precise location of the reattachment point was measured by four different methods such as oil dots, tufts, a single hot wire and a split film probe.

Velocity reversal characteristics in reattaching flows can be quantified by the forward-flow fraction, γ, which is defined as the fraction of time duration in which the flow is directed in the downstream direction. If γ equals 1, the fluid flows all the time in the downstream direction, whereas if γ equals zero, the flow is always in reverse direction.

The forward-flow fraction is measured using a split film sensor (Thermo-Systems Inc., model 1288) with two constant temperature anemometers (TSI, model 1050). The present method has been proposed by Ra et. al.(1990b) in which the experimental procedure is decribed in detail. For accurate measurement, the overheat ratios of two CTAs were carefully matched. The zero suppression and filtering of the CTA output signals were accomplished using two TSI 1057 signal conditioners. The split film plane of the sensor lies perpendicular to the floor wall. The output signals from the signal conditioners were digitized using a universal waveform analyzer (Data Precision, Data 6000) with a sampling frequency of 100 Hz. Then a total of 10 ensembles of 4096 data set were averaged and stored in an IBM PC/AT personal computer. The measured γ value has an uncertainty level of $\pm 2\%$ at 20 : 1 odds.

The wall static pressure distribution was measured by tapping 19 holes of 1 mm diameter along the centerline in the lower plate. The pressure signals were processed by an analog micromanometer (Furness P.P.F.A.FC060) which can measure as low as 0.01 mm Aq.

The streamwise and crosswise velocity components in a PWJ were measured using a constant temperature hot wire anemometer (KANOMAX, model 7224). The probe was X type, made of tungsten wire of diameter 5 μm and effective length 1.25 mm. The wire overheat ratio was 2.0 and the frequency response was set at 15 KHz. The probe was calibrated with the Collis and William's law and yaw tested, which gave $\Psi_1=42.5°$ and $\Psi_2=45.2°$. Since the variation in the ambient temperature was within ± 0.2°C during the experiments, temperature compensation was not made to the hot wire signals. The signals were linearized and then recorded on a magnetic tape recorder (Brüel and Kjaer, model 7003) at a tape speed of 15 inch/sec. The AC signal outputs from the tape recorder were low pass filtered at 10 KHz through a signal conditioner (TSI, model 1057) and then were processed by a turbulence processor (TSI, model 1015C) to obtain instantaneous values of u, v and the derivative $\tau(\partial u/\partial t)$, where τ is a time constant which was adjusted to attain optimum conditions for the derivative $\partial u/\partial t$(ref. TSI 1015C manual). These three analog signals were simultaneously converted to digital data of 14 bits by a digital data processor (Data Precision, M601) at a rate of 10 K samples per second for each channel.

Mean velocity vectors and Reynolds stresses in the high turbulence field including reverse flow region of the WAOJ were measured by a split film probe. A significantly favorable feature of the split film sensor over an X wire probe is its smaller physical size. This improves the spatial resolution in the region of large velocity gradient and allows two-dimensional turbulence quantities to be measured at a region much closer to a surface than is possible with the X wire probe. The split film sensor is also applicable to the flow field of much higher turbulence intensity than can be measured by the X wire probe because of its insensitiveness to the flow in the direction of sensor axis. Flow reversal can be measured by comparing the heat flux ratios of each film.

The split film probe was an end-flow type (0.15 mm diameter and 2 mm long), and it was calibrated at the exit of a jet from a calibration equipment (TSI, model 1125). The split film sensor was mounted on a rotating device to rotate the sensor

split plane in front of the jet. This allows the sensor to be calibrated for the angular response.

The performance of the split film sensor depends on the calibration scheme and the flow field. In the present study, the Stock's calibration scheme (Stock and Jaballa, 1985) was modified to achieve an improved pitch angle response independent of the flow velocity. Details of the calibration procedure were described in Ra et. al. (1990a). The proposed modified calibration scheme was verified by a reverse calibration experiment using the same apparatus. The experiment showed that the error in the maximum pitch angle at $\pm$ 70° is less than 5%, and the error in the mean velocity measurement by the split film is about $\pm$ 2% at the maximum calibration velocity of 30 m/s. For each points, 10 ensemble of 8192 data set were used to obtain the mean velocity and Reynolds stresses. The uncertainty estimates by the Kline and McClintock's(1953) method revealed that the error in the turbulent stresses is about 9% for the typical turbulent intensity of 10% and the error in the triple products is up to about $\pm$ 20% for its maximum value.

Now a discussion about the reliability of the split film measurements of mean velocity and turbulent stresses is in order. Following the pioneering work of Spencer and Jones(1971) on the split film sensor, there appeared a number of researches about its reliability. Kiya and Sasaki(1983, 1985) used the split film successfully to investigate the complex structure of a turbulent separation bubble. They showed that in regions of high turbulence the split film measurements are much more reliable than the measurements by the hot wire probe do. In the fully forward-flow region, u' measurements by the split film were slightly larger than those by the hot wire, whereas, the reverse is true for v' measurements. But, in the turbulent field with frequent flow reversals, the split film sensor out-performs over the hot wire probe. Stock and Jaballa(1985) also studied the capability of the split film sensor for turbulence measurements. They found a reverse trend to that observed by Kiya and Sasaki(1983, 1985) and also found that the streamwise fluctuation measurements in low turbulence by the split film were always 5 to 10 % lower than those by the hot wire. But both studies agreed that for turbulent flows with high intensity and flow reversals the split film sensor must be used instead of the hot wire.

Before the present experiment, the split film sensor was used to measure a backward-facing step flow by Ra et. al.(1990a). With a modified calibration scheme proposed in the paper, the mean velocity and streamwise fluctuations were obtained by the split film and the hot wire in the forward flow field zone without any discrepancy.

3. Results and Discussion

Flow visualization methods using oil dots and tufts were applied to identify the reattachment region. The oil dots and tufts were equally spaced along the downstream direction with an interval of 0.5 D, where D is the jet width. After determining the region of the reattachment point by these methods, more accurate location of the reattachment point was obtained by using a single hot wire technique, as has been suggested by Bergeles and Athanassiadis(1983). A single hot wire was scanned along the streamwise direction at a distance of 0.5 mm above the wall in the previously determined reattachment region. Then, the location of lowest the output signal was identified as the point of reattachment with an uncertainty of about 0.15 D, or 3 mm. The split film was also used to determine the reattachment point by measuring the downstream distribution of the forward-flow fraction at a distance 0.3 mm off the wall.

The reattachment is a very unsteady process, and the zone of reattachment is rather wide. Based on the measured distribution of the forward-flow fraction near the wall, γ_w, the point at which γ_w is 50% is considered as the time mean reattachment point of the unsteady reattaching flow where the mean skin friction coefficient vanishes approximately (see Eaton et. al.(1979) and Ra et. al. (1990b) for reliability of the present experimental procedure). Measurements of the probability distributions of the velocity fluctuations very-near the wall show that it is positively skewed just

downstream and negatively skewed just upstream of the reattachment. However, at the reattachment point, the probability distribution is very nearly symmetric. Therefore, it may be inferred that the point of $\gamma_W = 50\%$ coincides with the point of zero-wall friction as was pointed out by Eaton et. al.(1979).

Figure 2 represents the reattachment distance, X_R, for various non-dimensional offset distances, H/D. The reattachment regions in which flow reversal occurs are represented by a bar, I, and the cross symbol indicates the positions at which $\gamma_W = 50\%$. Although the present results are slightly larger than those of Bourque and Newman(1960) and Sawyer(1963), the linear dependence of the reattachment length on the offset distance for high H/D is consistent with that of the dimensional analysis of Bourque and Newman(1960). The γ measurement shows that the reattachment region increases with the offset distance.

Figure 3 shows the distribution of the forward-flow fraction, γ_W, along the wall in comparison with that in the reattachment region of a backward-facing step flow. Pronchick(1983) suggested the following distribution of the forward-flow fraction in the reattachment zone of a backward-facing step ;

$$\gamma_W(X^*) = \frac{1}{2}\{1 + sgn(X^*) erf(4.30\ X^*)\}$$

The γ_W distribution of the WAOJ is much narrower than that of the backward-facing step flow. This result implies that the length scale of large eddies in the impingement region of the WAOJ is smaller than that in the reattachment zone of the backward-facing step flow. If the numerical constant 4.30 in the above equation is changed to a value 15.2, Pronchicks' correlation equally well represents the present data of the WAOJ. For the smallest offset ratio of $H/D = 1.0$, the γ_W data are skewed in the negative direction.

The variations of pressure coeffcient along the wall are shown in Fig. 4. The wall suction pressure in the first half of the separated bubble region decreases to reach a minimum near the center of the bubble and then repidly increases to

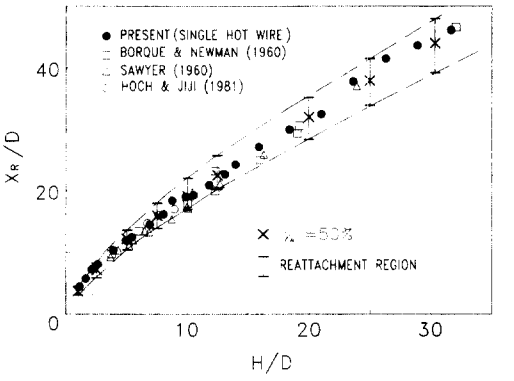

Fig. 2 Variation of the reattachment length as a function of the offset height

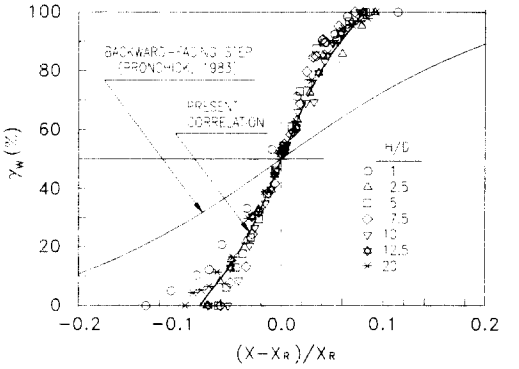

Fig. 3 Distribution of the forward-flow fraction ratio for various offset ratio

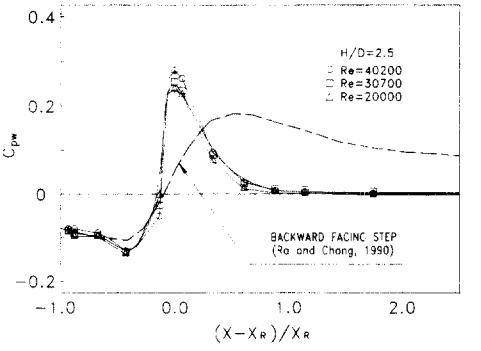

Fig. 4 Wall pressure distribution in wall-attaching offset jet for various Reynolds numbers

a positive peak at the reattachment point, which is in coincidence with the results for $H/D < 6.0$ by Kumada et. al.(1973) and Yoo et. al.(1986). In the figure C_{pw} is the wall pressure coefficient defined

as $C_{pw}=(P_w-P_\infty)/\frac{1}{2}\rho U_j^2$, where P_w is the wall pressure, P_∞ the ambient pressure, and ρ the density of air. The wall pressure distribution of a backward-facing step flow with zero pressure gradient in free stream is compared in the figure. The pressure recovery from the recirculating bubble of the WAOJ takes place much faster than that of the backward-facing step flow. The shortening of the pressure recovery zone comparing with the backward facing flow in Fig. 4 is closely related to the narrowing of the reattachment region in Fig. 3.

This point of positive peak surface pressure is often used as a theoretical criterion for the impingement point of the dividing streamline starting from the lower edge of the nozzle exit of a WAOJ (Hoch and Jiji, 1981). Hoch and Jiji(1981) assumed that the wall pressure in the reattachment region exhibits a similarity characteristic in an exponential form, $C_{pw}/C_{pm}=exp[-\beta(X-X_R)^2/H^2]$, where C_{pm} is the maximum wall pressure coefficient, and the pressure spread coefficient β was found to be 3.4. They asserted that this value is independent of the offset height H/D and the free stream velocity, U_∞ Fig. 5 compares the wall pressure variations near the impingement region obtained by a number of experimental investigators. Although each set of data seems to show such an exponential decay, the value of β varies rather widely with the experiments. This wide variation of β suggests that the flow field must depend on not only H/D but also the initial turbulence intensity, the inital exit boundary layer thickness ($\delta=0.874$ mm in our experiments), the aspect ratio, and the wall roughness, etc.. Among these parameters, the effect of the initial turbulence level has been vividly demonstrated by Nozaki et. al.(1981).

The mean velocity vector field in the initial flow development region of the WAOJ with $H/D=5.0$ is represented in Fig. 6. The time averaged zero-horizontal velocity line ($\gamma_w=50\%$) and the edge of the recirculating bubble ($\gamma_w=99\%$) are also plotted in the figure. The recirculation region can be observed with the vortex center approximately at about $X/D=7.5$. In the corner at which the offset plate and back wall intersect, the presence of a secondary vortex flow is inferred. The primary jet flow curves slowly through the

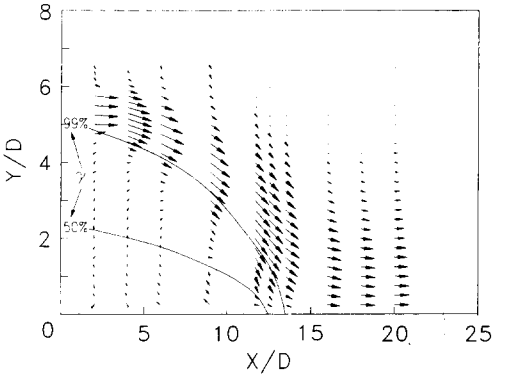

Fig. 6 Mean velocity vector profiles, H/D=5.0

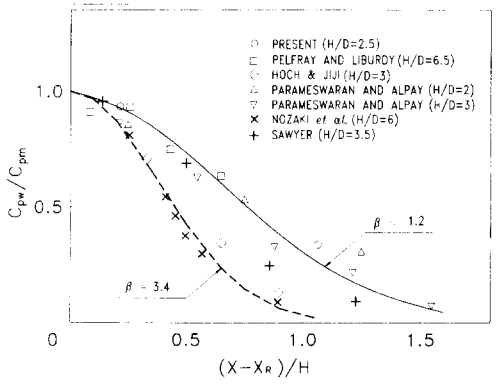

Fig. 5 Comparison of normalized wall pressure data with theory

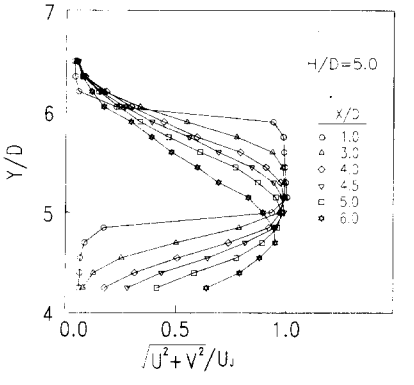

Fig. 7 Mean velocity distributions in the initial region, X/D≤10

first one third of the recirculating region and then turns sharply downward as the jet impinges on the offset plate. The same trend has been observed in backward-facing step flows, but the streamline starts to curve after half of the separated bubble region. The maximum reverse flow velocity of the WAOJ was about 37 percent of the jet exit velocity.

Distributions of the mean velocity magnitudes near the jet exit are shown in Fig. 7. If the length of the initial flow development region is defined as the downstream distance from the jet exit to the point where the magnitude of the local maximum mean velocity vector begins to decrease as defined by Rajaratnam(1976), the flow development region in the WAOJ extends up to about 4.5 D, which is similar to those of plane turbulent jets by Person(1981) and Everit and Robins(1978). As can be seen the figure, the jet development is immediately influenced by the recirculation region below the jet exit, as has been found by Pelfray and Liburdy(1986a).

To investigate any similarity between the WAOJ and the PWJ at far downstreams, the mean velocity profiles are non-dimensionalized by using the local maximum velocity and length scale, U_m and $Y_{\frac{1}{2}m}$ defined in Fig. 1, respectively, and the results are compared in Fig. 8. The solid lines in the figures are typical non-dimensionalized mean velocity profile in the self-preserving region of the PWJ. According to Rajaratnam and Subramanya(1968), the mean velocity profile of the PWJ becomes similar at the downstream distance greater than 20 D, which can be confirmed in Fig. 8b. Such similarity is also observed in the WAOJs at the downstream distance $X>3X_R$ in Fig. 8a. Considering the profiles near the end of the impingement region of the WAOJ ($X/D=10$ for $H/D=2.5$ and $X/D=16$ for $H/D=5.0$), the development into a similar profile seems to be rather fast.

The decays of the maximum axial velocity U_m of the WAOJ and the PWJ are displayed in log scales in Fig. 9, where other measurement data of the WAOJ by Hoch and Jiji(1981) are also included for comparison. It is interesting to note that the maximum velocity decay of the WAOJ

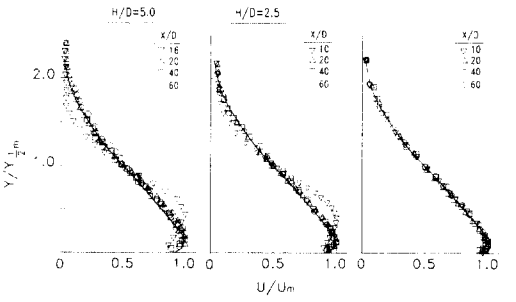

Fig. 8 Non-dimensional mean velocity distributions Wall-attaching offset jet and Plane wall jet

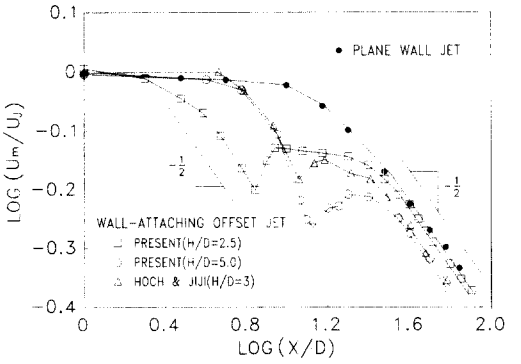

Fig. 9 Logarithmic plots of the maximum velocity variations to show power law decay

merges with that of the PWJ after $X/D=35$ or $\log(X/D)=1.54$. Within the experimental uncertainty, it may be concluded that the maximum velocity decay of the WAOJ, both in the initial development region and in the wall jet region, obey the conventional $-\frac{1}{2}$ power law of the PWJ.

Figure 10 depicts the upper jet spreads of the WAOJ and the PWJ; both jets grow linearly with the downstream distance. The linear spread rate is about 0.076, which falls in the previously reported range(0.065−0.081) of the linear spread rate of the PWJ (Rajaratnam, 1976). Pelfray and Liburdy(1986b) employed curvilinear coordinates η and ζ, where η is parallel with and ζ is normal to the maximum velocity vector at a given streamline position, to find the linear growth of the WAOJ with a high offset ratio of seven. However, in the present case of low offset height such linear

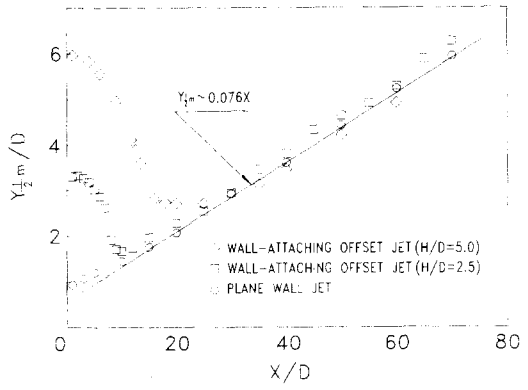

Fig. 10 Upper jet spreads of the wall-attaching offset jet and the plane wall jet

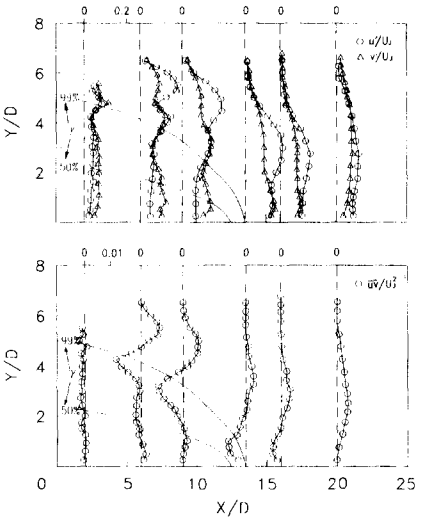

Fig. 11 Distributions of (a) turbulent component intensities and (b) Reynolds shear stress distributins

growth could be approximately observed in the usual $X-Y$ coordinates.

Dur to the highly turbulent flow nature of the impingement region, the conventional X wire measurements are inadequate to obtain turbulent quantities in the WAOJ flows except in the region far downstream after the point of reattachment. The turbulent quantities which will be described in the followings were obtained by using the split film probe.

Downstream variations of the turbulent intensity profiles (u'/U_J and v'/U_J) of the WAOJ with $H/D=5.0$ are demonstrated in Fig. 11. Due to the violent mixing process of the discharged jet with the surroundings, both intensity profiles before the reattachment have two peaks on both sides with respect to the jet center line. Such double-peaked profiles persist up to about $X/D \approx 15$ and then the double-peaks disappear in the wall jet region. The peak intensity grows and the region of high turbulence broadens as the jet develops. The peak turbulence intensity then decays, beginning somewhere in the reattachment zone. Due to the suction pressure field below the jet, the profiles are skewed toward the bottom plate. It is worth noting that the vertical component intensity v'/U_J is higher than the streamwise intensity u'/U_J But in the further downstream region, the streamwise component intensity remains much stronger than the vertical component.

The Reynolds shear stress distributions in the WAOJ are included in Fig. 11. In the upper part of the WAOJ, the Reynolds shear is positive and its local maximum value decreases with the downstream distance up to the reattachment point. However in the lower part of the jet, the Reynolds shear stress is negative. This implies that the momentum of the main jet stream is transferred downward into the recirculation bubble region.

In the impingement region, typified at $X/D=13$, a large downward momentum transfer still exists. In $X/D \geq 20$, the $\overline{uv}$ profile shapes are similar to those of the PWJ; both have negative values near the wall, and the positions of the maximum $\overline{uv}$ are nearly the same.

A feature of wall jets that has attracted considerable interests is that the zero crossing point of the shear stress profile does not coincide with the point of local maximum velocity. In the present experiments the point of zero crossing of the shear stress profile lies closer to the wall (about 54%) than the local maximum velocity position as the plane wall jet (61%, Irwin, 1973).

In order to investigate the similarity, the turbulent stresses in the wall jet region of the case $H/D=2.5$ are non-dimensionalized by the local length and velocity scales, $Y_{\frac{1}{2}m}$ and U_m, respectively, and the results are plotted in Fig. 12. The WAOJ attains the similarity slower than the PWJ.

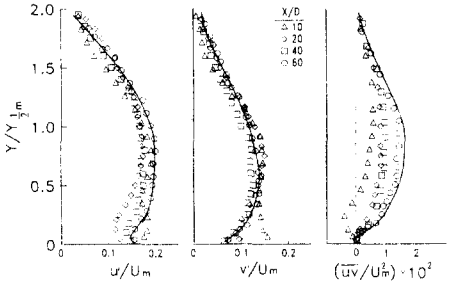

Fig. 12 Non-dimensional turbulent component intensities and Reynolds shear stress distributions in wall-attaching offset jet with plane jet (solid line)

The normal stresses u' and v' approach to those profiles of the PWJ in the measurement range. But the Reynolds stress $\overline{uv}$ of the WAOJ does not reach the similarity state even at $X/D=60$. The zero crossing of $\overline{uv}$ in the WAOJ at $X/D=60$ occurs at about $Y/Y_{\frac{1}{2}m}\approx 0.072$, which is a little lower than the value of 0.075 in the measurements of Guitton(1970) and Wilson and Goldstein (1976).

Figure 13 shows the variations of triple products, $\overline{u^3}$, $\overline{u^2v}$, $\overline{uv^2}$, and $\overline{v^3}$. Upstream of the reattachment point, all the triple product profiles in the mixing region between the jet and recirculation bubble are roughly antisymmetric as in a typical plane jet, but the peak values in the lower side are different from those in the upper side. The peak values increase with the jet development up to a half of the recirculating flow region where the streamline curvature is not significantly varied (Pelfray and Liburdy, 1986b) and then decrease as the highly curved jet impinges onto the wall. The stabilizing streamline curvature causes such decrease in the triple products. In the impingement region, the triple products $\overline{v^3}$ and $\overline{u^2v}$ have maxima at about one nozzle height above the offset plate and decrease more rapidly near the surface than in the outer region, presumably as a result of distortion of the large eddies by the constraint of the solid boundary. All the triple products except $\overline{u^3}$ in the reattachment zone change their shapes drastically near the solid surface due to the impingement of the main stream. The profiles of $\overline{u^3}$ vary in such a way that

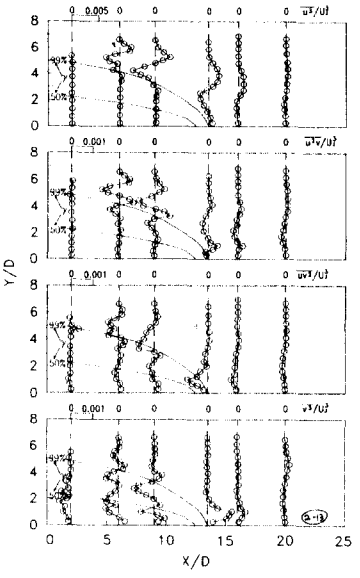

Fig. 13 Turbulent triple products distributions

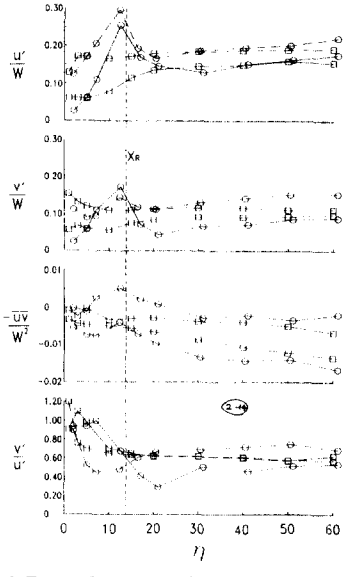

Fig. 14 Reynolds normal and shear stress versus η. W is local velocity magnitude, η is the distance from the nozzle exit along the local maximum velocities (solid line) and along the upper jet spread (dashed line) : ○, wall-attaching offset jet ; □, plane wall jet

their symmetry persist up to the end of reattachment zone, and then $\overline{u^3}$ decreases in magnitude with the zero crossing point moving downward. All the zero crossing lines of the triple products

are off from the maximum Reynolds stress position. Far downstream of the reattachment, the triple products decrease in the streamwise direction. At the last measurement station, the profiles of the triple products have roughly the same shape as those in a PWJ (not shown in this paper).

The variations of the Reynolds normal and shear stress along the maximum local velocity line and upper jet spread line are expressed in Fig. 14. Referring to Fig. 15 cited from Pelfray and Liburdy(1986b), the curvature stain rate defined as $-W/R$ where W is the local velocity magnitude and R is radius of curvature, is negative before a position of some distance ahead of the reattachment and then it becomes positive afterward, both along the two lines.

Theoretically, the turbulent stresses are augmented under the negative curvature strain rate (unstable state) and they decrease under the positive curvature strain rate (stable state). Figure 14 precisely shows such streamline curvature effect on the tubulent stresses in the region before the reattachment of the WAOJ. The crosswise velocity fluctuations are always less than the streamwise fluctuations and the ratios seem to approach to those of the PWJ far downstream of a value about 0.6. (Note, however, in the recirculation bubble v' is larger than u' as has been seen in Fig. 11.)

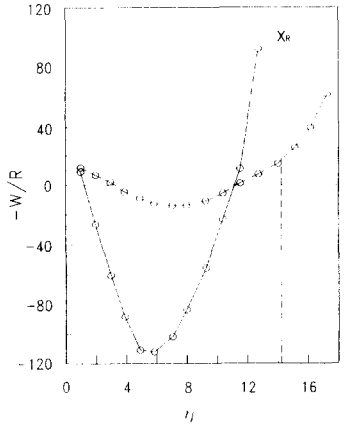

Fig. 15 Curvature strain rate, W/R versus η. η is the distance from the nozzle exit along the line of maximum velocities (solid line) and jet spread (dashed line) cited from Fig. 5 of Pelfray and Liburdy (1986b)

Due to the strong curvature effects in the recirculation zone (see Fig. 14) and anisotropic turbulent structures (see Figs. 11 and 12), it seems that the standard k-ϵ model is inadequate to use for the prediction of the WAOJ.

4. Conclusions

Comparative data of the turbulent field characteristics as well as the mean flow characteristics are provided for a wall attaching offset jet (WAOJ) and a plane wall jet(PWJ) respectively. Although the initial development region of the WAOJ is strongly affected by the suction pressure field in the recirculation bubble at the corner, the maximum velocity decay, the jet spread, and the turbulence field in the wall jet region are quite similar to those of the turbulent plane wall jet.

When the streamwise distance from the nozzle exit plane is used to represent the maximum velocity decay and the upper jet spread, there are virtually no differences between those of the WAOJ in the wall jet region and of the PWJ for the present offset ratio, $H/D=2.5$ and 5.0. The mean velocity field attains the similarity profile quite earlier than the Reynolds stresses do and of the Reynolds stresses the shear stress takes longest time to get the similarity.

The triple products change their shapes drastically with impingement process and then approach the typical profile of the self-preserving PWJ, but the values in the WAOJ ar still higher than those of the PWJ.

Development of turbulence along the streamwise coordinate η depending on the curvature strain rate showed that the turbulent kinetic energy increases before the reattachment due to destablizing effect of the streamline curvature in that region, and then it decreases due to the stabilizing streamline curvature afterward.

In addition, the variation of the reattachment length as a function of the offset ratio and the wall pressure distribution of the WAOJ are included to compare them with the theory and previous experimental data.

References

Bergeles, G. and Athanassiadis, N., 1983, "The Flow Past a Surface-Mounted Obstacle," ASME J. of Fluid Engr., Vol. 105, pp. 461~463.

Bourque, C. and Newman, G., 1960, "Reattachment of a Two-Dimensional, Incompressible Jet to an Adjacent Flat Plate," Aeron. Quar., Vol. 11, pp. 201~232.

Cebeci, T. and Bradshaw, P., 1977, "Momentum Transfer in Boundary Layer," McGraw-Hill, pp. 154~160.

Eaton, J. K., Jeans, A. H. and Johnston, J. P., 1979, "A Wall-Flow Direction Probe for Use in Separating and Reattaching Flows", Trans. ASME, J. Fluid Engr., Vol. 101, pp. 363~366.

Everitt, K. W. and Robins, A. G., 1978, "The Development and Structure of Turbulent Plane Jets," J. of Fluid Mech., Vol. 88, pp. 563~583.

Guitton, D. E., 1970, "Some Contributions to the Study of Equilibrium and Non-Equilibrium Wall Jets over Curved Surfaces," Ph. D. Thesis, McGill University.

Hoch, J. and Jiji, L. M., 1981, "Two-Dimensional Turbulent Offset Jet-Boundary Interaction," ASME J. of Fluid Engr. Vol. 103, pp. 154~161.

Irwin, H. P. A. H., 1973, "Measurements in a Self-Preserving Plane Wall Jet in a Positive Pressure Gradient," J. of Fluid Mech., Vol. 61. pp. 33~63.

Kiya, M. and Sasaki, K., 1983, "Structure of a Turbulent Separation Bubble," J. of Fluid Mech., Vol. 137, pp. 83~113.

Kiya, M. and Sasaki, K., 1985, "Structure of Large-Scale Vortices and Unsteady Reverse Flow in the Reattaching Zone of a Turbulent Separation Bubble," J. of Fluid Mech., Vol. 154, pp. 463~491.

Kline, S. J. and McClintock, F. A., 1953, "Describing Uncertainties in Single-Sample Experiments," Mechanical Engr., Vol. 5, pp. 3~8.

Kumada, M., Mabuchi, I. and Oyakawa, K., 1973, "Studies in Heat Transfer to Turbulent Jets with Adjacent Boundaries (3rd Report Mass Transfer to Plane Turbulent Jet Reattachment on an Offset Parallel Plate)," Bull. of JSME, Vol. 16, pp. 1712~1722.

Morel, T., 1977, "Design of Two-Dimensional Wind Tunnel Contractions," ASME J. of Fluid Engr., Vol. 99, pp. 371~378.

Nozaki, T., Hatta, K., Sato, N. and Matsumura, H., 1981, "Reattachment Flow Issuing from a Finite Width Nozzle (Report 2. Effects of Initial Turbulence Intensity)," Bull. of JSME, Vol. 24, pp. 363~369.

Parameswaran, V. and Alpay, S. A., 1975, "Studies on Re-Attaching Wall Jets," Trans. CSME, Vol. 3, pp. 83~89.

Pelfray, J. R. R., 1984, "Characteristics of a Turbulent Plane Offset Jet," Ph.D. Dissertation, Mech. Engr. Dept. Clemson University.

Pelfray, J. R. R. and Liburdy, J. A., 1984, "Turbulent Characteristics of an Offset Jet," 2nd International Symposium on Application of Laser Anemometry to fluid Mechanics.

Pelfray, J. R. R. and Liburdy, J. A., 1986a, "Mean Flow Characteristics of a Turbulent Offset Jet," ASME J. of Fluid Engr., Vol. 108, pp. 82~88.

Pelfray, J. R. R. and Liburdy, J. A., 1986b, "Effect of Curvature on the Turbulence of a Two-Dimensional Jet," Exp. Fluids, Vol. 4, pp. 143~149.

Persen, L. N., 1981, "The Near Feld of a Plane Turbulent Jet," Fluid Dynamics of Jets with Application of V/STOL, AGARD Conference Proceedings. No. 308.

Pronchick, S. W., 1983, "An Experimental Investigation of the Structure of a Turbulent Reattaching Flow Behind a Backward-Facing Step," Ph. D. Thesis, Dept. of Mech. Eng., Stanford University

Ra, S. H. and Chang, P. K., 1990, "Effects of Pressure Gressure Gradient on Reattaching Flow Downstream of a Rearward-Facing Step," J. Aircraft, Vol. 27, pp. 93~95.

Ra, S. H., Chang, P. K. and Park, S. O., 1990a, "A Modified Calibration Technique for the Split Film Sensor," Meas. Sci. Technol., Vol. 1, pp. 1156~1161.

Ra, S. H., Chang, P. K. and Park, S. O., 1990b, "Measurement of the Forward-Flow Fraction

Using a Split Film Sensor," Exp. Fluids, Vol. 10, pp. 57~59.

Rajaratnam, N., 1976, "Turbulent Jets," Elsevior Scientific Publishing Company, pp. 211~225.

Rajaratnam, N. and Subramanya, N., 1968, "Plane Turbulent Reattached Wall Jets", ASCE J. of Hydraulics Div., Vol. 94, pp. 95~112.

Sawyer, R. A., 1960, "The Flow Due to a Two-Dimensional Jet Issuing Parallel to a Flat Plate," J. of Fluid Mech., Vol. 9, pp. 543~560.

Sawyer, R. A., 1963, "Two-Dimensional Reattaching Jet Flows Including the Effect of Curvature on Entrainment," J. of Fluid Mech., Vol. 17. pp. 481~498.

Spencer, B. W. and Jones, B. G., 1971, "Turbulence Measurements with the Split Film Anemometer Probe," Proc. Symp. on Turbulence in Liquids, University of Missouri, Rolla. pp. 7~15.

Stock, D. E. and Jaballa, T. M., 1985, "Turbulence Measurements Using Split Film Anemometry," Proc. Int. Symp. on Refined Flow Modelling and Turbulence Measurement (University of Iowa) H15-1-10.

Tritton, D. J., 1977, "Physical Fluid Dynamics," Van Nostrand Reinhold Company, pp. 284~286.

Wilson, D. J. and Goldstein, R. J., 1976, "Turbulent Wall Jets with Cylindrical Streamwise Surface Curvature," ASME J. of Fluid Engr., Vol. 98, pp. 550~557.

Yoo, J. Y., Kang, S. H., Chae, S. K. and Choa, S. H., 1986, "A Study on the Plane Turbulent Offset Jet," Trans. of KSME, Vol. 10, No. 3, pp. 357~366.